Received: 12 October 2017 | Revised: 8 January 2018 | Accepted: 5 February 2018

DOI: 10.1002/mrm.27154

PRECLINICAL AND CLINICAL SPECTROSCOPY

Magnetic Resonance in Medicine

Rapid Communication

In vivo hyperpolarization transfer in a clinical MRI scanner

Cornelius von Morze[1] | Galen D. Reed[2] | Peder E. Larson[1] | Daniele Mammoli[1] | Albert P. Chen[2] | James Tropp[3] | Mark Van Criekinge[1] | Michael A. Ohliger[1] | John Kurhanewicz[1] | Daniel B. Vigneron[1] | Matthew E. Merritt[4]

[1] Department of Radiology and Biomedical Imaging, University of California, San Francisco, California

[2] GE Healthcare, Dallas, Texas

[3] Berkshire Magnetics, Berkeley, California

[4] Department of Biochemistry, University of Florida, Gainesville, Florida

Correspondence
Cornelius von Morze, Department of Radiology and Biomedical Imaging, University of California, San Francisco, 1700 Fourth Street, Byers Hall Suite 102, San Francisco, CA 94158, USA.
Email: cornelius.vonmorze@ucsf.edu

Funding information
NIH K01DK099451 (CVM), P41EB013598 (DBV), R01DK105346 (MM), R01HD087306 (MM), R01DK112865 (MM), P41GM122698 (MM), U24DK097209 (MM), and NSF/DMR1644779 (MM)

Purpose: The purpose of this study was to investigate the feasibility of in vivo ^{13}C->^{1}H hyperpolarization transfer, which has significant potential advantages for detecting the distribution and metabolism of hyperpolarized ^{13}C probes in a clinical MRI scanner.

Methods: A standalone pulsed ^{13}C RF transmit channel was developed for operation in conjunction with the standard ^{1}H channel of a clinical 3T MRI scanner. Pulse sequences for ^{13}C power calibration and polarization transfer were programmed on the external hardware and integrated with a customized water-suppressed ^{1}H MRS acquisition running in parallel on the scanner. The newly developed RF system was tested in both phantom and in vivo polarization transfer experiments in $^{1}J_{CH}$-coupled systems: phantom experiments in thermally polarized and hyperpolarized [2-^{13}C] glycerol, and ^{1}H detection of [2-^{13}C]lactate generated from hyperpolarized [2-^{13}C] pyruvate in rat liver in vivo.

Results: Operation of the custom pulsed ^{13}C RF channel resulted in effective ^{13}C->^{1}H hyperpolarization transfer, as confirmed by the characteristic antiphase appearance of ^{1}H-detected, $^{1}J_{CH}$-coupled doublets. In conjunction with a pulse sequence providing 190-fold water suppression in vivo, ^{1}H detection of hyperpolarized [2-^{13}C]lactate generated in vivo was achieved in a rat liver slice.

Conclusion: The results show clear feasibility for effective ^{13}C->^{1}H hyperpolarization transfer in a clinical MRI scanner with customized heteronuclear RF system.

KEYWORDS
dynamic nuclear polarization, INEPT, lactate, pyruvate

1 | INTRODUCTION

Hyperpolarized (HP) ^{13}C MRI, based on the method of dissolution dynamic nuclear polarization,[1,2] is currently undergoing translation into studies of human disease.[3,4] Localized metabolic activity of injected HP ^{13}C probes can be tracked via ^{13}C MRI, by exploiting chemical shift differences among metabolites. Numerous technical investigations have focused on strategies for optimally sampling the spatial-spectral distribution of the transient HP ^{13}C magnetization (reviewed in Ref 5. Although nearly all of the previous in vivo work has focused on direct detection, shifting the hyperpolarization from ^{13}C nuclei to nearby ^{1}H spins offers significant potential advantages for detecting and imaging the in vivo

distributions and metabolic transformations of HP ^{13}C probes. These include theoretically increased sensitivity of detection and reduced requirements on imaging gradient areas, both of which are caused by the approximate 4-times higher gyromagnetic ratio of ^{1}H versus ^{13}C. Moreover, in this approach, specialized ^{13}C receiver coils and electronics are supplanted by standard ^{1}H equipment, which more readily attains body noise dominance at the higher readout frequency,[6] and potentially simplifies HP ^{13}C MRI acquisition, as ^{1}H coils are already tightly integrated with well-developed MRI acquisition methods including parallel imaging.[7,8]

Building on previous work in vitro,[9–12] initial preclinical studies have reported the feasibility of in vivo ^{13}C->^{1}H hyperpolarization transfer using the method of insensitive nuclei enhanced by polarization transfer (INEPT).[13–15] However, although such sequences are widely implemented on NMR spectrometers and preclinical MRI systems, clinical MRI systems are not generally configured for heteronuclear polarization transfer experiments. In this work, we have developed a supplementary standalone pulsed ^{13}C RF channel to operate simultaneously with ^{1}H spectroscopic acquisition on a clinical 3T MRI scanner, thus facilitating ^{13}C->^{1}H polarization transfer using a simplified reverse INEPT-type sequence. The newly developed clinical hardware/software framework was applied for ^{13}C->^{1}H HP transfer in $^{1}J_{CH}$-coupled systems in both phantom and in vivo experiments: phantom ^{1}H MR experiments in thermally polarized and HP [2-^{13}C]glycerol, and ^{1}H detection of HP [2-^{13}C]lactate generated from HP [2-^{13}C]pyruvate by enzymatic transformation via lactate dehydrogenase in normal rat liver in vivo.

2 | METHODS

2.1 | Development of a supplementary pulsed ^{13}C RF transmit channel

A commercial standalone 3T ^{1}H decoupler (GE Healthcare, Waukesha, WI) [16] was modified extensively to instead operate in a pulsed mode at ^{13}C Larmor frequencies, whereas the standard system ^{1}H RF channel was used simultaneously for ^{1}H transmit/receive. The apparatus consisted of 3 main rack-mounted components: a Herley model 3445 RF amplifier with 2-kW pulsed peak power and frequency range 10 to 130 MHz (Ultra Electronics Herley, Lancaster, PA), an Agilent model E4438C (option package 601) vector electronic signal generator (ESG) with frequency range of 250kHz- to 6 GHz (Agilent Technologies, Santa Clara, CA), and a Windows PC equipped with an Agilent model 82357A universal serial bus (USB)/general purpose input output (GPIO) interface used for controlling the ESG. The purpose of the USB/GPIO interface is to carry waveform instructions from the USB port of the PC to the GPIO port of the ESG.

Software provided by the vendor to control the ESG from the PC, based on the Agilent VEE programming environment, was bypassed by directly issuing commands over the USB/GPIO connection using a custom software interface programmed in MATLAB (MathWorks, Natick, MA). The commands used the syntax of Standard Commands for Programmable Instruments, which is supported by the ESG. This custom software interface allowed arbitrary complex RF waveforms (i.e., the ^{13}C pulse sequence) to be loaded onto the ESG at arbitrary carrier frequencies and power levels, and to be played with arbitrary timing delays with respect to a transistor-transistor-logic (TTL) trigger signal received from the MRI scanner. The TTL signal from the scanner exciter board goes high during signal readout, and was fed to an external trigger port of the ESG to trigger the ^{13}C pulse sequence at a specified delay after the start of the previous ^{1}H readout. The custom software that was written to enable generation of external RF pulses on the Agilent ESG, timed with synchronization to a MRI scanner pulse sequence, is available for download from MATLAB File Exchange at https://www.mathworks.com/matlabcentral/fileexchange/65372-cvonmorze-external-rf-mri, which is linked to the corresponding source code repository on GitHub.

For ^{1}H decoupling,[17] the amplifier operates in a continuous-wave mode without any RF blanking, with irradiation provided continuously at 2 separate power levels during readouts and the intervals between readouts (to facilitate nuclear Overhauser enhancement, although this is not generally useful for the case of HP studies). Two highly selective frequency filters, placed in series, ensure that application of ^{1}H decoupling power does not interfere with ^{13}C detection. These filters were uninstalled for the purpose of the pulsed MR experiments described in this study. Instead, the amplifier was configured for RF blanking during readout intervals, using the same readout trigger that was also used for timing the execution of the ^{13}C pulse sequence. As described, because the TTL signal precisely marks the readout intervals, blanking of the amplifier was achieved by simply feeding the TTL trigger signal to the blanking input on the amplifier (which is designed to blank when the input is high), in addition to the external trigger port of the ESG.

The external RF system architecture is illustrated in Figure 1. ^{13}C pulse power was delivered using low-loss LMR-400 coaxial cabling from the output of the RF amplifier through a bulkhead connector panel located in the rear of the scanner room and into 1 of 2 linear modes of the ^{13}C channel (i.e., the 0° ^{13}C port) of a dual-tuned $^{13}C/^{1}H$ volume quadrature transceiver coil (inner diameter = 4 cm, length = 8 cm), whose quadrature ^{1}H channel was connected as usual to the 3T clinical MRI scanner. For calibration of the external ^{13}C pulse power, the resulting ^{13}C MR signal was detected using the other linear mode (i.e., the 90° ^{13}C port), which was connected to the 3T MRI scanner. Although this

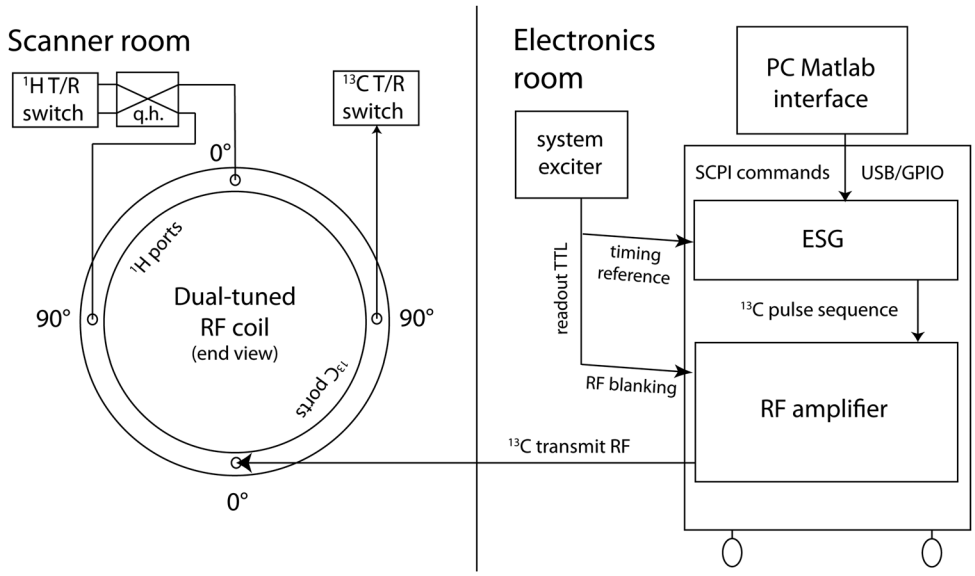

FIGURE 1 System diagram for operation of supplementary ^{13}C RF transmit channel in conjunction with ^{1}H MRS on the clinical MRI scanner. The ^{13}C pulse sequence is executed on the independent electronic signal generator (ESG), which is programmed from a PC interface and timed with respect to a transistor-transistor-logic (TTL) signal from the system exciter board. Following amplification, ^{13}C transmit RF power is coupled into 1 of the 2 linear modes of the quadrature ^{13}C channel of a dual-tuned volume coil, whereas the other mode is coupled to the scanner ^{13}C receiver for the purpose of power calibration. The coil ^{1}H channel is connected to the ^{1}H transmit/receive (T/R) switch as usual through a quadrature hybrid (q.h.). SCPI, Standard Commands for Programmable Instruments; USB/GPIO, universal serial bus/general purpose input output

scheme requires twice the transmit power to attain a given flip angle as compared with quadrature excitation, it facilitated ^{13}C detection for direct calibration of the external pulse power, whereas the standard excitation by the MR scanner system RF was temporarily deactivated in software. A manufacturer-supplied "white noise" pickup coil circuit, which deactivates the receivers in the event of detection of extraneous RF power, was temporarily disabled for the purpose of all experiments involving externally supplied RF power. No attempt was made to synchronize RF phase between ^{1}H and ^{13}C channels.

2.2 | ^{13}C pulse sequences

Two ^{13}C RF pulse sequences were programmed in MATLAB to run on the ESG. One served for ^{13}C pulse power calibration, and the other for ^{13}C->^{1}H polarization transfer. The power calibration sequence consisted of a single 500-μs hard pulse. The polarization transfer sequence (Figure 2) consisted of 2 consecutive 500-μs hard pulses with 90° RF phase shift, with pulse centers separated by 3.33 ms, or approximately $1/(2^{1}J_{CH}) = 1/(300\,\text{Hz})$.[13] In addition to RF blanking the amplifier during signal readout, the ESG was also blanked outside of the pulse sequence execution intervals (i.e., no carrier signal was detectable at the output of the ESG). Each sequence was triggered to execute just before the signal readout on the subsequent TR interval on the MRI scanner, using a programmed delay following the scanner TTL signal, marking the beginning of the first MR signal readout. For both sequences, the exact timing of the pulse sequence with respect to MR signal readout was verified by monitoring RF amplifier output and scanner TTL trigger signals on a Tektronix model TDS5034B oscilloscope (Tektronix, Beaverton, OR). For power calibration, a 1-mL vial containing 6-M aqueous [^{13}C]urea and 1% 500-mM Gd-DTPA (v/v) was excited with TR = 5 seconds. The results were used to determine the 90° ^{13}C power level.

2.3 | Product operator description of polarization transfer sequence

A product operator analysis of the applied pulse sequence considering a J-coupled, ^{1}H-^{13}C spin pair is straightforward and does not differ substantially from the original INEPT analysis.[13] The initial $90°_x$ excitation pulse produces pure phase $-I_y$ coherence, which then evolves under the scalar J-coupling. With the evolution delay set to $1/(2\,J_{CH})$ (3.33 ms), the I_y coherence is transformed into a bilinear coherence with an amplitude scaled by the gyromagnetic ratio of ^{13}C as well as the dynamic nuclear polarization enhancement (*Enh*):

$$Enh \cdot \gamma_C I_{C_z} \xrightarrow{I_{C_x}(90)} -Enh \cdot \gamma_C I_{C_y} \xrightarrow{\pi J \tau 2 I_{H_z} C_z} -Enh \cdot \gamma_C 2 I_{H_z} I_{C_x} \quad (1)$$

After the hard $90°_y$ pulse on the ^{13}C channel, the antiphase magnetization is restored to the Z-axis, where the subsequent ^{1}H-shaped pulse produces a $H_{xy}C_z$ bilinear coherence that will be transformed into pure ^{1}H coherence after a further 1/(2 J) evolution period. The phase of the

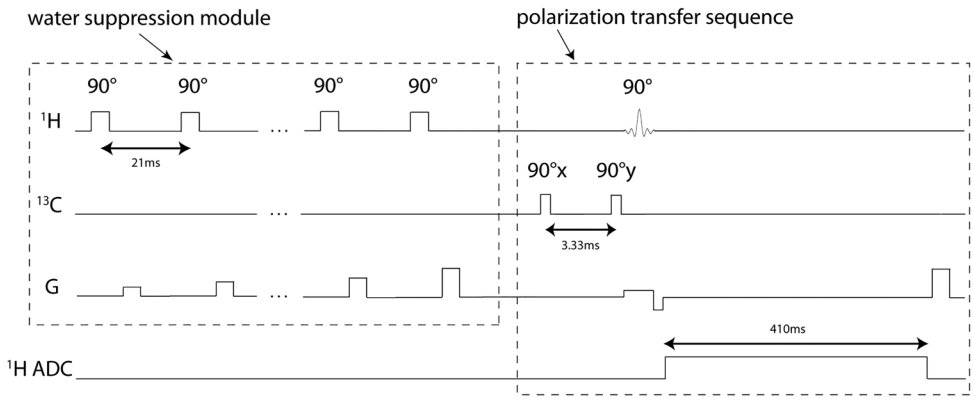

FIGURE 2 Pulse sequence diagram for $^{13}C->^{1}H$ hyperpolarization transfer in vivo. The sequence consists of a 3-pulse, simplified insensitive nuclei enhanced by polarization transfer (INEPT) type polarization transfer sequence (right dotted box), preceeded by a water-suppression module (left dotted box) consisting of 10 consecutive 90° RF pulses with attendant spoiler gradients. The ^{1}H T/R used the standard system RF channel, and the ^{13}C RF power was supplied by the external system

transverse ^{1}H bilinear term can be modulated by switching the phase of the ^{1}H readout pulse. As the transverse ^{1}H coherence is generated initially from an antiphase coherence, the enhanced signal will be an antiphase doublet without phase correction. Because this is a true polarization transfer, the enhancement of the ^{1}H signal intensity is scaled by $\gamma(^{13}C)/\gamma)^{1}H)$ (i.e., a measured enhancement of 10 000 for a ^{13}C detected experiment can only produce an enhancement of 2500 for ^{1}H after INEPT transfer). The sequence as implemented neglects the 180° pulses on both the ^{1}H and ^{13}C channels, as normally used, as both the ^{1}H and ^{13}C resonances were placed directly on resonance. Without the constraints of broadband polarization transfer, the sequence as implemented is considerably simpler than refocused versions of INEPT. In our implementation, the slight temporal offset between the near-simultaneous ^{13}C and ^{1}H pulses does not change the analysis of the sequence significantly.

2.4 | Water suppression sequence

Suppression of endogenous water signal is critical for ^{1}H detection of transferred hyperpolarization in vivo. To this end, a custom spectrally selective water-suppression module[18] was programmed for the ^{1}H MRS sequence on the MRI scanner, which consisted of a train of 10 consecutive 90° maximum-phase Shinnar-LeRoux pulses[19] with attendant spoiler gradient pulses. Although spectral selectivity was not required, the suppression sequence was adapted from a module that was originally designed for selective quenching of specific HP ^{13}C resonances,[20] and therefore used spectrally selective RF pulses (pulse width = 13 ms) centered on the water peak. For the in vivo experiments, this suppression train was executed at the beginning of each TR interval, just before ^{1}H excitation and detection. A delay of 8 ms was appended to the end of the pulse train to allow a window for execution of the ^{13}C sequence before ^{1}H excitation/readout. The degree of water suppression that could practically be achieved using this sequence was measured in vivo in a normal rat.

2.5 | Magnetic resonance experiments

To test the basic feasibility of $^{13}C->^{1}H$ hyperpolarization transfer using this custom setup, we first hyperpolarized 30 μL of [2-^{13}C]glycerol (Cambridge Isotopes, Tewksbury, MA), mixed with 15 mM of trityl radical OX063, in a commercial Hypersense dissolution dynamic nuclear polarizer operating at 1.3 K and 3.35 T with approximately 94.1-GHz microwave irradiation (Oxford Instruments, Tubney Woods, UK). Following buildup of hyperpolarization, the solid sample was rapidly dissolved in 5 mL of superheated D_2O to obtain a solution of 80-mM HP [2-^{13}C]glycerol and transferred to the MRI scanner. ^{13}C hyperpolarization was transferred to the proton attached to the labeled carbon using the described polarization transfer sequence running on the external hardware, alongside the ^{1}H MR spectroscopy sequence running on the scanner. The sequence was executed twice with TR = 1 second, with the first readout triggering execution of the external ^{13}C 90°x-90°y sequence just before the second readout. On the ^{1}H side, excitation was by a single 500-μs 90° hard pulse, with a subsequent readout of 2048 points and 5 kHz sweep width. The ^{13}C sequence was completed approximately 200 μs before the ^{1}H excitation pulse. We also repeated the same polarization transfer experiment using a vial phantom containing 3 g of thermally polarized [2-^{13}C]glycerol.

Next, the potential for ^{1}H detection of [2-^{13}C]lactate generated from HP [2-^{13}C]pyruvate in vivo was tested in a normal Sprague Dawley rat. Animal experiments were conducted in accordance with a protocol approved by the Institutional Animal Care and Use Committee. The rat was anesthetized using inhalational isoflurane (1.5%, 1-L/minute

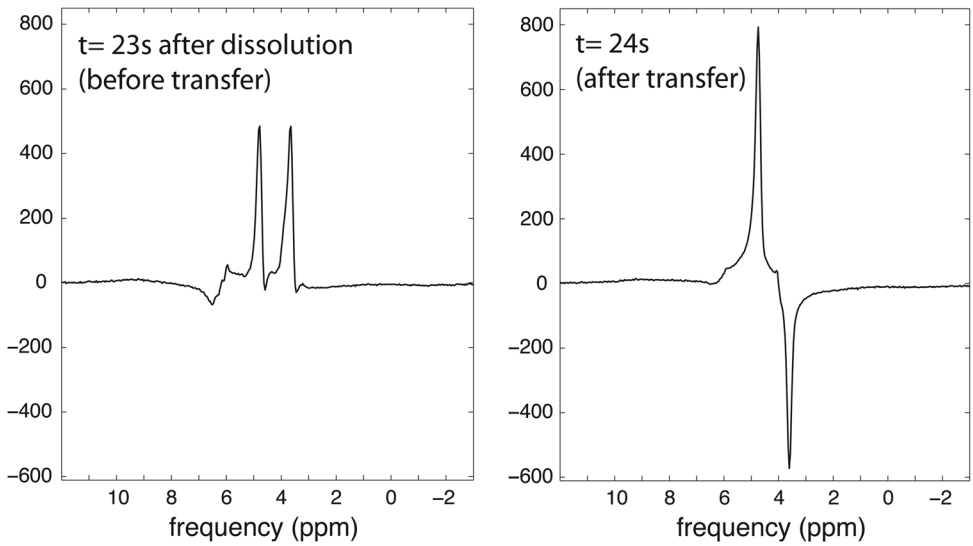

FIGURE 3 Phased ^{1}H MR spectra (real) of HP [2-^{13}C]glycerol phantom collected on first (left) and second (right) TR intervals of the described polarization transfer sequence. The second spectrum clearly showed an antiphase appearance that is characteristic of polarization transfer, as described. The y-axes are scaled to units of approximate SNR

O_2 flow rate), with lateral tail vein catheter implanted before imaging. The MR acquisition was identical to the phantom experiment except for 2 key differences: (1) The water suppression module was appended to the beginning of each TR of the pulse sequence; and (2) Instead of ^{1}H hard pulse excitation, an 8-mm axial ^{1}H slice through the rat liver was excited with center frequency on water, using a slice-selective 1.8-ms windowed sinc pulse excitation. The ^{13}C sequence timing was adjusted so that it again completed approximately 200 μs before the ^{1}H excitation pulse. For the HP experiment, 24 μL of [2-^{13}C]pyruvic acid was hyperpolarized via dynamic nuclear polarization and subsequently dissolved in 4.6 mL of 80-mM NaOH/Tris buffer. The resulting 80 mM of HP [2-^{13}C]pyruvate sample was injected over 12 seconds, and the MR acquisition sequence was started 25 seconds after the start of injection. To stimulate the exchange of the HP label into the lactate pool, an equimolar quantity of sodium lactate (natural abundance) was co-injected at the same time as the HP [2-^{13}C]pyruvate.[21,22]

3 | RESULTS

Operation of the newly developed, external pulsed ^{13}C RF transmit system in conjunction with ^{1}H spectroscopic acquisition on the clinical scanner resulted in effective ^{13}C->^{1}H hyperpolarization transfer. Polarization transfer in the HP [2-^{13}C]glycerol phantom was evidenced by the characteristic antiphase appearance of the resulting ^{1}H signal doublet on the second readout (Figure 3), following execution of the ^{13}C sequence. Initial ^{1}H hyperpolarization of this doublet (in-phase) was also observed on the first readout, an effect that is probably caused by cross relaxation,[23] but was largely extinguished by the first ^{1}H excitation. On the second TR, the SNR for each half of the detected signal doublet was in excess of 500:1. Because of the time required to transport the HP sample to the MRI scanner, the MR pulse sequence could not be started until 23 seconds after the start of the dissolution. Since the ^{13}C T_1 relaxation time of [2-^{13}C]glycerol was separately measured to be approximately 7 seconds in D_2O at 3 T, we estimate that approximately 96% of the initial polarization was lost before MR data acquisition. Nevertheless, this experiment shows clear feasibility for polarization transfer using the described MRI system configuration. We also confirmed the efficacy of polarization transfer in the thermally polarized phantom containing [2-^{13}C]glycerol, noting an antiphase shift in the intensities of the ^{13}C-coupled ^{1}H doublet (Figure 4). The effect is much more subtle in this case, when transferring only the tiny thermal polarization of ^{13}C, but very clear on the difference spectra.

Transfer of hyperpolarization was also evident in the in vivo rat experiment using HP [2-^{13}C]pyruvate. In this case, the hyperpolarization of [2-^{13}C]lactate generated enzymatically in vivo from HP [2-^{13}C]pyruvate via lactate dehydrogenase was transferred to the directly bonded proton. In contrast to the phantom experiment, which was purposefully conducted in D_2O, water suppression was critical for the detection of polarization transfer in vivo. Application of the water-suppression module resulted in 190-fold suppression of the endogenous water signal in the rat liver slice, based on comparing the area under the water peak with and without the suppression sequence. Slice selection for ^{1}H MRS resulted in much better water suppression as compared with the nonselective mode (approximate 20-fold increase), because of the greater B_1 homogeneity over the slice. Similar to the phantom results, a resonance corresponding to

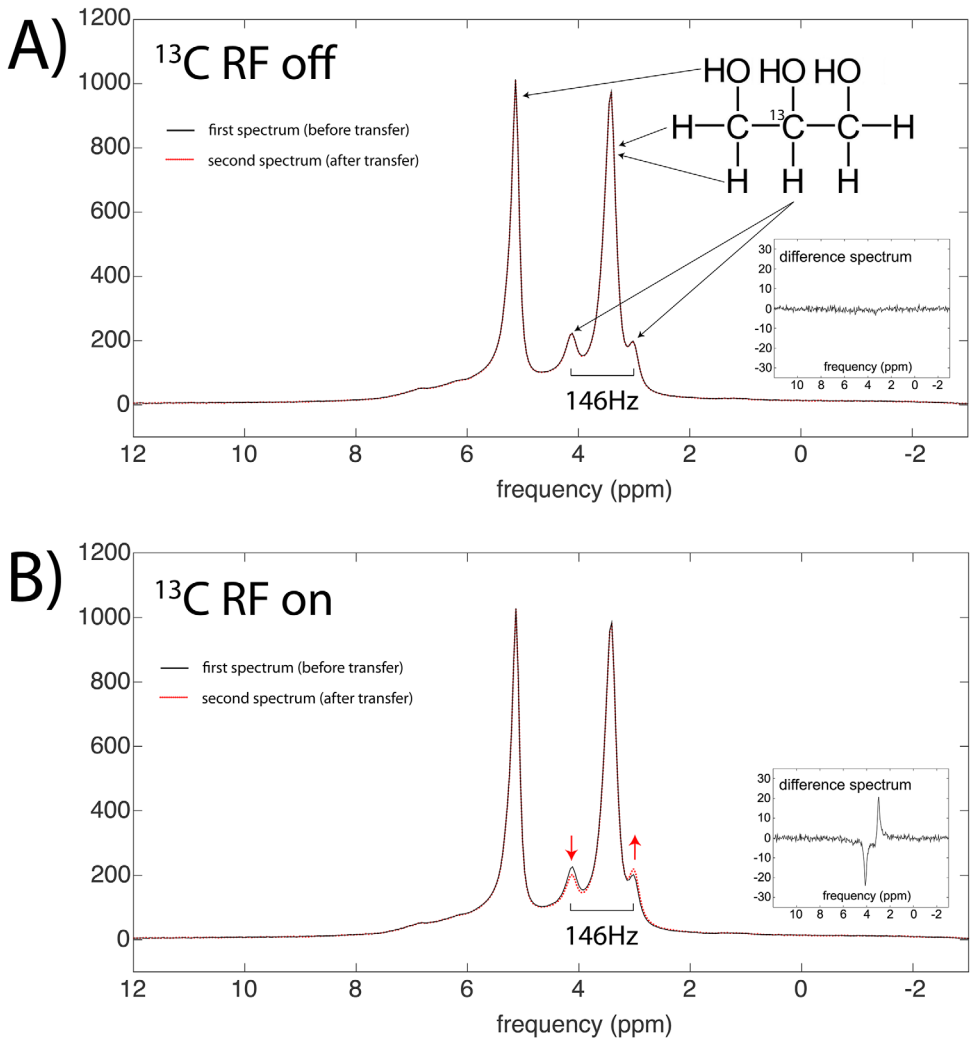

FIGURE 4 Phased ^{1}H MR spectra (real) of thermally polarized [2-^{13}C]glycerol vial phantom. A subtle antiphase shift in the intensities of the ^{13}C-coupled ^{1}H doublet is observed when the polarization transfer sequence is executed (B), but not when the external ^{13}C RF is deactivated (A). A pair of red arrows highlight the directionality of the shift. In each case, the spectra acquired before (solid black line) and after (red dotted line) the transfer sequence are shown superimposed on a single axis. Difference spectra are shown as insets

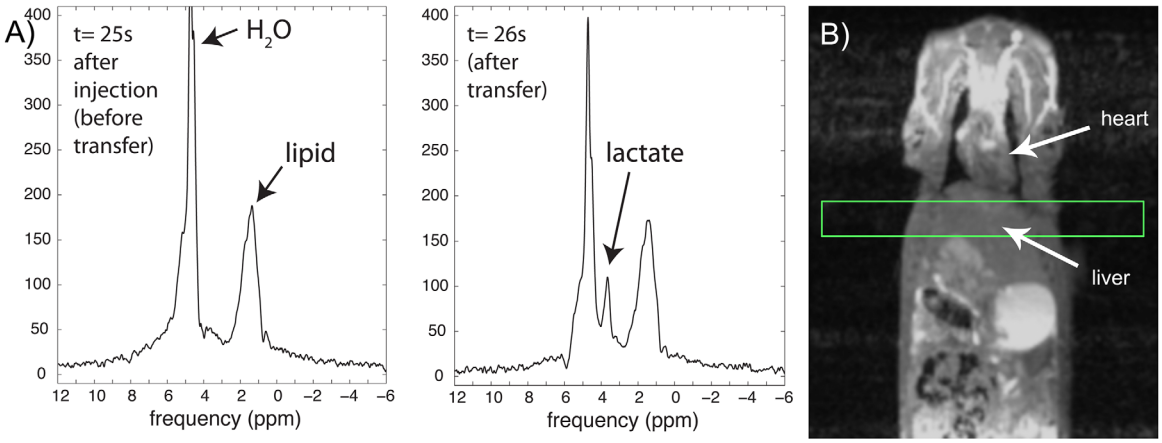

FIGURE 5 A, In vivo localized ^{1}H detection of HP [2-^{13}C]lactate generated from [2-^{13}C]pyruvate in an 8-mm axial slice through rat liver. The ^{1}H lactate peak appeared after the polarization transfer sequence was executed during the second TR interval (right panel of [A]). Magnitude spectra are shown. B, Position of the axial slice, overlaid on a coronal anatomic ^{1}H MRI image

transferred HP lactate clearly appeared on the second ^{1}H MRS readout (Figure 5), following execution of the ^{13}C sequence. Despite effective water suppression, the other half of the ^{1}H lactate doublet could not be detected, probably because it was swamped by the large water peak.

4 | DISCUSSION

Our results extend into a clinical MRI scanner environment prior initial reports demonstrating the feasibility of in vivo ^{13}C->^{1}H hyperpolarization transfer.[14,15] This functionality was enabled by developing an external pulsed ^{13}C RF transmit channel, for operation in conjunction with a water-suppressed, localized ^{1}H MRS acquisition sequence running in parallel on the scanner. An alternate, potentially easier, approach could be to modify the scanner system itself to support simultaneous multinuclear excitation, if it can support this mode. At least 2 previous studies have described scanner system changes along these lines. Gordon et al enabled simultaneous imaging of HP ^{13}C and ^{1}H nuclei on a 4.7T preclinical system.[24] Wild et al re-engineered a 3T clinical scanner to support near-simultaneous imaging of 3 different nuclei (HP ^{3}He and ^{129}Xe, as well as ^{1}H).[25] The present study is the first to our knowledge to enable hyperpolarization transfer in a clinical system. The customized external RF system has potential advantages of increased flexibility and vendor neutrality. The key additional hardware required for our external approach is a vector RF ESG and RF amplifier. Approximate cost estimates for these 2 components are \$20 000 to \$30 000 for a new high-end RF ESG that is comparable to the model used in this study, and \$25 000 to \$50 000 for a RF amplifier with comparable output power and performance. Alternatively, a MRI system equipped with a secondary "broadband" amplifier dedicated to non-^{1}H studies could easily be modified for driving with an external ESG. Custom software is also required for this approach. We have successfully programmed one external ESG (Agilent) for the purpose of timed MRI pulse generation, and we are freely distributing the source code online.

In contrast to a recent study showing the feasibility of in vivo polarization transfer from HP [1-^{13}C]lactate (generated in vivo from [1-^{13}C]pyruvate) to its distant methyl protons (with $J_{CH} = 4.1$ Hz),[15] much larger couplings (approximately 150 Hz) characterize the $^{1}J_{CH}$ systems investigated in this work ([2-^{13}C]glycerol and [2-^{13}C]lactate). This case has the significant advantage of much shorter required evolution times, which go with $1/J_{CH}$, therefore minimizing the loss of polarization as a result of T_2 decay during the transfer process. Furthermore, the refocusing pulses necessary for standard INEPT acquisition are not required in this case, as $(1/J_{CH}) << T_2^*$. Another consideration when comparing the 2 systems is that the ^{13}C T_1 relaxation times of the $^{1}J_{CH}$-coupled species are also much shorter than [1-^{13}C]lactate as a result of larger dipolar coupling, which increases together with the larger J-coupling, potentially resulting in greater loss of polarization prior to transfer. This is not a fundamental limitation of our approach, however, as the lifetime of the HP metabolic product is much less important than its (relatively unaffected) precursor. In contrast to the HP precursor molecule, which is subject to a long delay period during transit and delivery to the target tissue of interest, the lifetime of the HP metabolic product need only be sufficiently long for its detection immediately after it is generated. Finally, it is important to also note that a short additional delay would be required to match the in-phase condition for the transferred doublet, in conjunction with ^{13}C decoupling to collapse it to a singlet. For proof of principle, however, the antiphase doublet provides valuable experimental proof for the efficacy of polarization transfer, in contrast with hyperpolarization of this proton via cross-relaxation.[23]

Although the described water-suppression scheme was sufficiently effective (providing 190-fold suppression) to facilitate detection of transferred HP ^{1}H lactate signal, the other half of the signal doublet could not be detected, probably because of residual interference from water signal. For this initial work, we have adopted a relatively basic water-suppression scheme consisting of a 90° pulse train. Future work will focus on improving the effectiveness of water suppression, likely using a combination of RF and gradient-enhanced approaches. We anticipate that a high degree of suppression should be feasible by application of coherence-selection gradients.[26] The basic principle of this approach is to apply different gradient areas to the transverse magnetization before and after polarization transfer, according to the difference in gyromagnetic ratios between the 2 nuclei. In this manner, gradients are balanced only for transferred magnetization, resulting in near-ideal suppression of background signal. Lipid suppression may also be important for some transfer targets, such as the methyl group protons in [1-^{13}C] lactate. In future studies, we will also aim to investigate the potential dynamic ^{1}H imaging of hyperpolarization transferred from ^{13}C, by implementing spectrally selective pulses on the external hardware with flip angles under 90°, so as to efficiently sample the magnetization dynamically.

ORCID

Cornelius von Morze http://orcid.org/0000-0002-3992-1793
Peder E. Larson http://orcid.org/0000-0003-4183-3634
Matthew E. Merritt http://orcid.org/0000-0003-4617-9651

REFERENCES

[1] Ardenkjaer-Larsen JH, Fridlund B, Gram A, et al. Increase in signal-to-noise ratio of >10,000 times in liquid-state NMR. *Proc Natl Acad Sci U S A*. 2003;100:10158-10163.

[2] Ardenkjaer-Larsen JH, Leach AM, Clarke N, Urbahn J, Anderson D, Skloss TW. Dynamic nuclear polarization polarizer for sterile use intent Rizi R, editor. *NMR Biomed.* 2011;24:927-932.

[3] Nelson SJ, Kurhanewicz J, Vigneron DB, et al. Metabolic imaging of patients with prostate cancer using hyperpolarized [1-C-13]pyruvate. *Sci Transl Med*. 2013;5:198ra108

[4] Cunningham CH, Lau JY, Chen AP, et al. Hyperpolarized 13C metabolic MRI of the human heart: initial experience. *Circ Res.* 2016;119:1177-1182.

[5] Cho A, Lau JYC, Geraghty BJ, Cunningham CH, Keshari KR. Noninvasive interrogation of cancer metabolism with hyperpolarized (13)C MRI. *J Nucl Med.* 2017;58:1201-1206.

[6] Edelstein WA, Glover GH, Hardy CJ, Redington RW. The intrinsic signal-to-noise ratio in NMR imaging. *Magn Reson Med.* 1986;3:604-618.

[7] Sodickson DK, Manning WJ. Simultaneous acquisition of spatial harmonics (SMASH): fast imaging with radiofrequency coil arrays. *Magn Reson Med.* 1997;38:591-603.

[8] Pruessmann KP, Weiger M, Scheidegger MB, Boesiger P. SENSE: sensitivity encoding for fast MRI. *Magn Reson Med.* 1999;42:952-962.

[9] Frydman L, Blazina D. Ultrafast two-dimensional nuclear magnetic resonance spectroscopy of hyperpolarized solutions. *Nat Phys.* 2007;3:415-419.

[10] Sarkar R, Comment A, Vasos PR, et al. Proton NMR of 15N-choline metabolites enhanced by dynamic nuclear polarization. *J Am Chem Soc.* 2009;131:16014-16015.

[11] Chekmenev EY, Norton VA, Weitekamp DP, Bhattacharya P. Hyperpolarized 1H NMR employing low γ nucleus for spin polarization storage. *J Am Chem Soc.* 2009;131:3164-3165.

[12] Dzien P, Fages A, Jona G, Brindle KM, Schwaiger M, Frydman L. Following metabolism in living microorganisms by hyperpolarized 1H NMR. *J Am Chem Soc.* 2016;138:12278-12286.

[13] Morris GA, Freeman R. Enhancement of nuclear magnetic resonance signals by polarization transfer. *J Am Chem Soc.* 1979; 101:760-762.

[14] Mishkovsky M, Cheng T, Comment A, Gruetter R. Localized in vivo hyperpolarization transfer sequences. *Magn Reson Med.* 2012;68:349-352.

[15] Wang J, Kreis F, Wright AJ, Hesketh RL, Levitt MH, Brindle KM. Dynamic ^{1}H imaging of hyperpolarized [1-^{13}C]lactate in vivo using a reverse INEPT experiment. *Magn Reson Med.* 2018;79:741-747.

[16] Chen AP, Tropp J, Hurd RE, et al. In vivo hyperpolarized 13C MR spectroscopic imaging with 1H decoupling. *J Magn Reson.* 2009;197:100-106.

[17] de Graaf RA, Rothman DL, Behar KL. State of the art direct ^{13}C and indirect ^{1}H-[^{13}C] NMR spectroscopy in vivo. A practical guide Rizi R, editor. *NMR Biomed.* 2011;24:958-972.

[18] Haase A, Frahm J, Hanicke W, Matthaei D. 1H NMR chemical shift selective (CHESS) imaging. *Phys Med Biol.* 1985;30:341-344.

[19] Pauly J, Le Roux P, Nishimura D, Macovski A. Parameter relations for the Shinnar-Le Roux selective excitation pulse design algorithm [NMR imaging]. *IEEE Trans Med Imaging.* 1991;10:53-65.

[20] von Morze C, Chang G-Y, Larson PEZ, et al. Detection of localized changes in the metabolism of hyperpolarized gluconeogenic precursors ^{13}C-lactate and ^{13}C-pyruvate in kidney and liver. *Magn Reson Med*. 2017;77:1429-1437.

[21] Day SE, Kettunen MI, Gallagher FA, et al. Detecting tumor response to treatment using hyperpolarized 13C magnetic resonance imaging and spectroscopy. *Nat Med.* 2007;13:1382-1387.

[22] Hurd RE, Spielman D, Josan S, Yen Y-F, Pfefferbaum A, Mayer D. Exchange-linked dissolution agents in dissolution-DNP ^{13}C metabolic imaging. *Magn Reson Med.* 2013;70:936-942.

[23] Merritt ME, Harrison C, Mander W, Malloy CR, Sherry AD. Dipolar cross-relaxation modulates signal amplitudes in the ^{1}H NMR spectrum of hyperpolarized [^{13}C]formate. *J Magn Reson.* 2007;189:280-285.

[24] Gordon JW, Fain SB, Niles DJ, Ludwig KD, Johnson KM, Peterson ET. Simultaneous imaging of 13C metabolism and 1H structure: technical considerations and potential applications. *NMR Biomed.* 2015;28:576-582.

[25] Wild JM, Marshall H, Xu X, et al. Simultaneous imaging of lung structure and function with triple-nuclear hybrid MR imaging. *Radiology* 2013;267:251-255.

[26] Ruiz-Cabello J, Vuister GW, Moonen CTW, van Gelderen P, Cohen JS, van Zijl PCM. Gradient-enhanced heteronuclear correlation spectroscopy: theory and experimental aspects. *J Magn Reson.* 2011;213:446-466.

How to cite this article: von Morze C, Reed GD, Larson PE, et al. In vivo hyperpolarization transfer in a clinical MRI scanner. *Magn Reson Med*. 2018;80:480–487. https://doi.org/10.1002/mrm.27154